**ORIGINAL ARTICLE**

# Predictive value of multiple metabolic and heterogeneity parameters of $^{18}$F-FDG PET/CT for EGFR mutations in non-small cell lung cancer

Aiqi Shi[1,2,3] · Jianling Wang[1,2,3] · Yuzhu Wang[1,2,3] · Guorong Guo[1,2,3] · Chouchou Fan[1,2,3] · Jiangyan Liu[1,2,3]

## Abstract

**Objectives** To explore the value of multiple metabolic and heterogeneity parameters of 2-deoxy-2-[fluorine-18] fluoro-D-glucose positron emission tomography/computed tomography ($^{18}$F-FDG PET/CT) in predicting epidermal growth factor receptor gene (EGFR) mutations in non-small cell lung cancer (NSCLC).

**Materials and methods** A retrospective analysis was performed by reviewing 98 patients with NSCLC who underwent EGFR mutation testing and $^{18}$F-FDG PET/CT examination in our hospital between March 2016 and March 2021. Patients were divided into an EGFR-mutant group and a wild-type group. A multivariate logistic regression analysis was performed to screen and construct a prediction model. The diagnostic performance of the model was evaluated using a receiver-operating characteristic (ROC) curve.

**Results** The study found that EGFR mutations were more likely to occur in women, non-smokers, and patients with peripheral lesions, shorter maximum tumor diameter, adenocarcinoma, and T1 stage cancer. Low maximum standardized uptake value (SUVmax), mean standardized uptake value (SUVmean), metabolic tumor volume, total lesion glycolysis, and high coefficient of variation (COV) were significantly correlated with EGFR mutations, and the area under the ROC curve (AUC) was 0.622, 0.638, 0.679, 0.687, and 0.672, respectively. Multivariate logistic regression analysis indicated that non-smokers (odds ratio (OR) = 0.109, $P$ = 0.014), peripheral lesions (OR = 6.917, $P$ = 0.022), low SUVmax ($\leq$ 7.85, OR = 5.471, $P$ = 0.001), SUVmean ($\leq$ 5.34, OR = 0.044, $P$ = 0.000), and high COV ($\geq$ 106.08, OR = 0.996, $P$ = 0.045) were independent predictors of EGFR mutations. The AUC of the prediction model established by combining the above factors was 0.926; the diagnostic efficiency was significantly higher than that of a single parameter.

**Conclusion** Among the metabolic and heterogeneity parameters of $^{18}$F-FDG PET/CT, low SUVmax, SUVmean, and high COV were significantly associated with EGFR mutations, and the predictive value of EGFR mutations could be enhanced when combined with clinicopathological features.

**Keywords** Non-small cell lung cancer · 2-Deoxy-2-[fluorine-18] fluoro-D-glucose positron emission tomography/computed tomography · SUVmax · Epidermal growth factor receptor

**Abbreviations**

| | |
|---|---|
| $^{18}$F-FDG PET/CT | 2-Deoxy-2-[fluorine-18] fluoro-D-glucose positron emission tomography/computed tomography |
| EGFR | Epidermal growth factor receptor |
| NSCLC | Non-small cell lung cancer |
| ROC | Receiver operating characteristic |
| TKI | Tyrosine kinase inhibitor |
| ROI | Region of interest |
| COV | Coefficient of variation |
| SD | Standard deviation |
| NOX4 | NADPH oxidase 4 |
| ROS | Reactive oxygen species |

✉ Jiangyan Liu
ery_liujy@lzu.edu.cn

1   Department of Nuclear Medicine, Lanzhou University Second Hospital, Chengguan District, Cuiyingmen No. 82, Lanzhou 730030, People's Republic of China

2   Second Clinical School, Lanzhou University, Lanzhou 730030, People's Republic of China

3   Key Laboratory of Medical Imaging of Gansu Province, Lanzhou 730030, People's Republic of China

| GLUT1 | Glucose transporter protein 1 |
| TNM | Tumor-node-metastasis |

## Introduction

Global cancer statistics show that the morbidity and mortality rates of lung cancer are the highest in men but lower than those in women with breast cancer [1]. The proportion of non-small cell lung cancer (NSCLC) is more than 85%, and adenocarcinoma is the predominant histologic subtype. A previous study reported a 5-year follow-up survival rate of only 17% [2]. Epidermal growth factor receptor gene (*EGFR*) mutations occur in approximately 20–50% of patients with NSCLC. In recent years, tyrosine kinase inhibitors (TKIs) have been shown to be effective in prolonging the survival of patients with EGFR mutations [3]. Therefore, EGFR detection is essential to guide clinical treatment. However, it is challenging to obtain satisfactory specimens due to various factors. Therefore, it is important to develop a simple and non-invasive method to assess the mutational status of EGFR.

2-Deoxy-2-[fluorine-18] fluoro-D-glucose positron emission tomography/computed tomography ($^{18}$F-FDG PET/CT), which combines anatomical and functional information, has been widely used in the diagnosis and treatment of lung cancer because of its non-invasive nature. The relationship between $^{18}$F-FDG PET/CT metabolic features and EGFR mutations is currently a hot topic in recent research. The maximum standardized uptake value (SUVmax) has been analyzed, but the results are still highly controversial. Furthermore, there have been few reports on mean standardized uptake value (SUVmean), metabolic tumor volume (MTV), and total lesion glycolysis (TLG), and the findings have been inconsistent.

Intratumoral heterogeneity is a crucial manifestation of tumor development and refers to the molecular biology or genetic changes in the process of evolution, which leads to differences in the rapid growth, invasiveness, and drug sensitivity of tumor cells [4, 5]. Intratumoral metabolic heterogeneity evaluated by $^{18}$F-FDG PET/CT has been studied in nasopharyngeal carcinoma, breast cancer, and NSCLC in some aspects [6–9], but a few studies have been performed on *EGFR* mutations. Therefore, this study aimed to analyze the correlation between intratumoral metabolic and heterogeneity parameters reflected by $^{18}$F-FDG PET/CT and EGFR mutations in patients with NSCLC, to explore the independent predictors of mutation, and to establish a predictive model to help guide clinical practice.

## Materials and methods

### Patient selection

A total of 98 patients diagnosed with NSCLC were retrospectively enrolled and underwent $^{18}$F-FDG PET/CT examination and *EGFR* testing at our hospital between March 2016 and March 2021. Of these, 83 had adenocarcinomas and 15 had non-adenocarcinomas (11 squamous carcinomas, 3 adenosquamous carcinomas, and 1 large cell carcinoma). The inclusion criteria were pathologically confirmed NSCLC; no antitumor treatment (such as surgery, radiotherapy, or others) before PET/CT examination; a time interval of less than 1 month between PET/CT and *EGFR* testing; and complete clinical and imaging data. The exclusion criteria were as follows: having received any form of antitumor therapy before the examination, a history of other malignancies, multiple primary lesions, and a primary lesion with a maximum diameter of 1 cm or less. Clinical data such as sex, age, smoking history, TNM stage, location, maximum diameter, CT margin signs, pathological type, and Ki67 index were recorded. The TNM stage was based on the lung cancer staging of the American Association for Cancer Research, 8th edition [10]. Patients were classified into mutant and wild-type groups according to the status of EGFR mutations, and the mutation group included 19, 20, and 21 subtype mutations. The study complies with the principles of the Declaration of Helsinki, and the work has been approved by the ethics committee of our institution. The requirement of obtaining written informed consent was waived because of the retrospective nature of the study.

### PET/CT acquisition and analysis

PET/CT was performed using a Discovery 690 imaging machine (GE Healthcare, WI, USA). The tracer used was $^{18}$F-FDG, which was produced by a medical cyclotron (MINItracer Qilin, GE Healthcare, WI, USA) and synthesized using an automated synthesis module. Radiochemical purity exceeded 95%. The patients fasted for at least 6 h before the examination. Blood glucose was confirmed to be less than 9.0 mmol/L before the intravenous injection of $^{18}$F-FDG at a dose of 2.96–5.55 MBq/kg. Imaging scanning was performed in the supine position after approximately 60 min of rest, ranging from the top of the head to the upper femur at 5–8 min per bed for the head and 3 min per bed for the rest of the regions. Attenuation-correction CT was performed using the following parameters: 120 kV, 50–220 mA, and 3.75 mm collimation. PET image acquisition was performed in static time of

flight + 3D mode, with an image matrix of $256 \times 256$. The reconstructed images were post-processed and fused using a MedEx (Beijing Madix) workstation to obtain PET, CT, and PET/CT fusion images at different levels.

The images were analyzed by two experienced nuclear medicine diagnosticians at the MedEx workstation. The maximum diameter referred to the maximum lesion diameter. According to the location of lung cancer, the lesions were divided into central and peripheral lesions. Central lesions referred to lung cancer occurring in lung segment and bronchus above lung segment, and peripheral lesions occurred in the bronchi below the lung segment. Positive CT margin signs were defined as the presence of at least one of the following three signs: spiculated sign, lobulated sign, and pleural indentation sign; negative signs were defined as the absence of all three signs. The primary lesion was identified by visual observation in the MedEx workstation, and the region of interest (ROI) was outlined around the lesion by surrounding the entire lesion with a threshold of 40% SUVmax. The relevant semi-quantitative metabolic parameters for quantifying $^{18}$F-FDG uptake values were subsequently derived from the software by automatically segmenting the lesion volumetrically in the cross-sectional, coronal, and sagittal planes. SUVmax was defined as the highest pixel value calculated using the following formula: SUVmax = maximum pixel activity/ (injected dose/ body weight). SUVmean is the mean value of pixel SUV. MTV was measured as the metabolic volume of the tumor with an ROI ≥ 40% SUVmax. TLG was calculated by multiplying MTV by SUVmean. The coefficient of variation (COV) was a PET/CT semi-quantitative parameter reflecting intratumor metabolic heterogeneity and was calculated as follows [7]:

$$COV = Standard\ deviation\ (SD)\ of\ SUV/\ SUVmean\ \times\ 100.$$

### EGFR mutation detection

EGFR mutation was detected by the pathology department of our hospital, and specimens were obtained through surgical resection, bronchoscopy, or puncture biopsy. The mutation status was analyzed using the polymerase chain reaction-based amplification-refractory mutation system and the EGFR mutation detection kit (Beijing SinoMD Gene Detection Technology Co., Ltd, Beijing, China).

### Statistical analysis

Statistical analysis was performed using SPSS software (version 23.0) and MedCalc software (version 19.0.4). Continuous variables were analyzed using Student's $t$ test and Wilcoxon rank-sum test, and the results are expressed as mean ± SD. The Chi-square test was used to compare categorical variables between the two groups, and the results are expressed as percentages. The best cut-off value was determined using the Jordan index. Multivariate logistic regression analysis was used to screen independent predictors and then combined independent predictors to construct a logistic regression model to evaluate the association between clinical and PET-related factors with EGFR mutation. After applying the model, a predicted probability of EGFR mutation status in each patient was obtained and its AUC was calculated. The DeLong test was used to compare the differences between receiver-operating characteristic (ROC) curves. A two-sided $P$ value of less than 0.05 was considered statistically significant.

## Results

### Patient characteristics

A total of 98 patients were eligible for the final analysis (55 men and 43 women). Among them, 55 patients (52 with adenocarcinoma; 94.5%) had EGFR mutations, while 43 patients (31 with adenocarcinoma; 72.1%) had wild-type mutations. The mean age of the two groups was $57.2 \pm 8.9$ and $58.4 \pm 9.5$ years, respectively. The majority of mutation subtypes were the exon 19 deletion ($n = 27$), followed by the L858R point mutation in exon 21 ($n = 25$) and other mutations ($n = 3$). There were 52 ever-smokers and 46 never-smokers. The clinical characteristics of the patients are summarized in Table 1.

### Association between clinical characteristics and EGFR mutations

Univariate analysis showed that EGFR mutations were more likely to occur in women, non-smokers, and patients with adenocarcinoma, peripheral lesions, shorter maximum tumor diameter, and T1 stage cancer, and the differences between the groups were statistically significant ($P < 0.05$), while the remaining indicators (age, N/M stage, clinical stage, and CT margin signs) were not significantly different. The dominant mutation subtypes in this study were exon 19 and 21 mutations, and the comparison of the above indicators between the two subtypes revealed no significant differences.

### Association between PET/CT parameters and EGFR mutations

SUVmax, SUVmean, MTV, and TLG were lower in the mutant group than in the wild group (9.02 vs 10.18, 5.20 vs 5.86, 6.09 vs 24.65, and 31.27 vs 141.50, $P = 0.038$, 0.019, 0.002, 0.002, respectively), but COV was higher in the mutant group (129.58 vs 99.86, $P = 0.004$), and the

**Table 1** Relationship between clinical features and EGFR mutations

| Characteristics | EGFR Wild ($n=43$) | EGFR Mutant ($n=55$) | $P$ |
|---|---|---|---|
| Age (years) | 58.4±9.5 | 57.2±8.9 | 0.523 |
| Gender (*n*, %) | | | 0 |
|   Male | 35 (81.4) | 20 (36.4) | |
|   Female | 8 (18.6) | 35 (63.6) | |
| Smoking history (*n*, %) | | | 0 |
|   No | 10 (23.3) | 36 (65.5) | |
|   Yes | 33 (76.7) | 19 (34.5) | |
| Location (*n*, %) | | | 0.004 |
|   Central | 15 (34.9) | 6 (10.9) | |
|   Peripheral | 28 (65.1) | 49 (89.1) | |
|   Maximum diameter (mm) | 39 (26, 59) | 29 (20, 38) | 0.005 |
| Pathological type (*n*, %) | | | 0.002 |
|   Adenocarcinoma | 31 (72.1) | 52 (94.5) | |
|   Non-adenocarcinoma | 12 (27.9) | 3 (5.5) | |
| T stage (*n*, %) | | | 0.009 |
|   1 | 15 (34.9) | 31 (56.4) | |
|   2 | 12 (27.9) | 17 (30.9) | |
|   3 | 11 (25.6) | 4 (7.3) | |
|   4 | 5 (11.6) | 3 (5.5) | |
| N stage (*n*, %) | | | 0.859 |
|   0 | 24 (55.8) | 30 (54.5) | |
|   1 | 7 (16.3) | 10 (18.2) | |
|   2 | 6 (14.0) | 5 (9.1) | |
|   3 | 6 (14.0) | 10 (18.2) | |
| M stage (*n*, %) | | | 0.785 |
|   0 | 27 (62.8) | 36 (65.5) | |
|   1 | 16 (37.2) | 19 (34.5) | |
| Clinical stage (*n*, %) | | | 0.839 |
|   I/II | 21 (48.8) | 28 (50.9) | |
|   III/IV | 22 (51.2) | 27 (49.1) | |
| Ki67 (*n*, %) | | | 0.154 |
|   ≤25% | 12 (27.9) | 23 (41.8) | |
|   >25% | 31 (72.1) | 32 (58.2) | |
| CT marginal sign (*n*, %) | | | 0.417 |
|   Yes | 28 (65.1) | 40 (72.7) | |
|   No | 15 (34.9) | 15 (27.3) | |

differences were statistically significant. ROC curve analysis revealed that the cut-off points for these parameters were 7.85, 5.34, 22.19, 103.55, and 106.08, corresponding to AUCs of 0.622, 0.638, 0.679, 0.687, and 0.672, respectively. However, the above parameters were not statistically different in mutant subtype analysis.
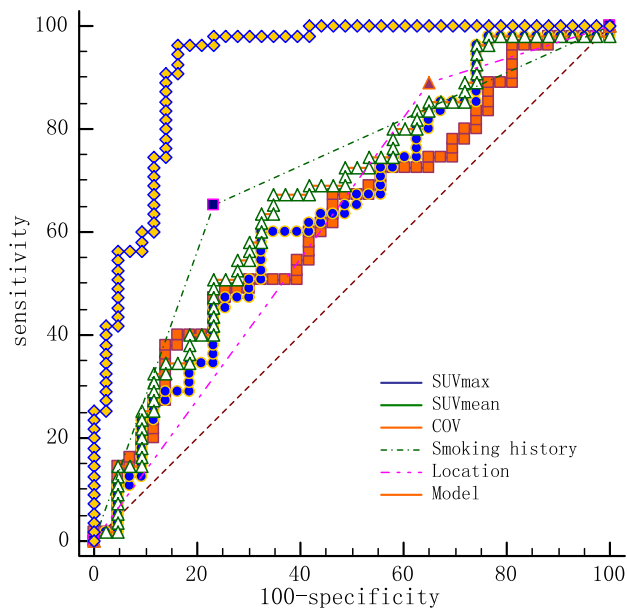
## Prediction of EGFR mutations

Factors with significant differences in the univariate analysis were incorporated into the multivariate logistic regression analysis, which revealed that smoking history, tumor location, SUVmax, SUVmean, and COV were independent

**Table 2** Multivariate analysis for the association between significant index and EGFR mutation

| Characteristics | Odds ratio | 95% CI | $P$ |
|---|---|---|---|
| Smoking history | 0.109 | 0.019~0.634 | 0.014 |
| Location | 6.917 | 1.318~36.307 | 0.022 |
| SUVmax | 5.471 | 1.980~15.114 | 0.001 |
| SUVmean | 0.044 | 0.008~0.243 | 0.000 |
| COV | 0.996 | 0.992~1.000 | 0.045 |

predictors of EGFR mutation (Table 2). These five factors were combined to construct a prediction model. Additionally, an ROC curve analysis was conducted to assess

the predictive value of the model, which showed that the AUC was 0.926 (cut-off: 0.441; 95% confidence interval: 0.870–0.981, sensitivity: 96.4%; specificity: 83.7%; positive predictive value: 89.1%; negative predictive value: 86.0%; and percentage correct: 87.8%). The diagnostic efficacy was significantly improved when compared to a single parameter, and the DeLong test showed statistically significant differences ($P < 0.0001$) between the five factors and the prediction model (Fig. 1). Representative images of $^{18}$F-FDG uptake in different EGFR mutation statuses are shown in Figs. 2 and 3.

## Discussion

EGFR mutations have been identified as one of the most common potential therapeutic targets for the treatment of NSCLC patients, and the implementation of effective EGFR–TKI therapy requires the early identification of appropriate patients. However, using tumor tissues or body
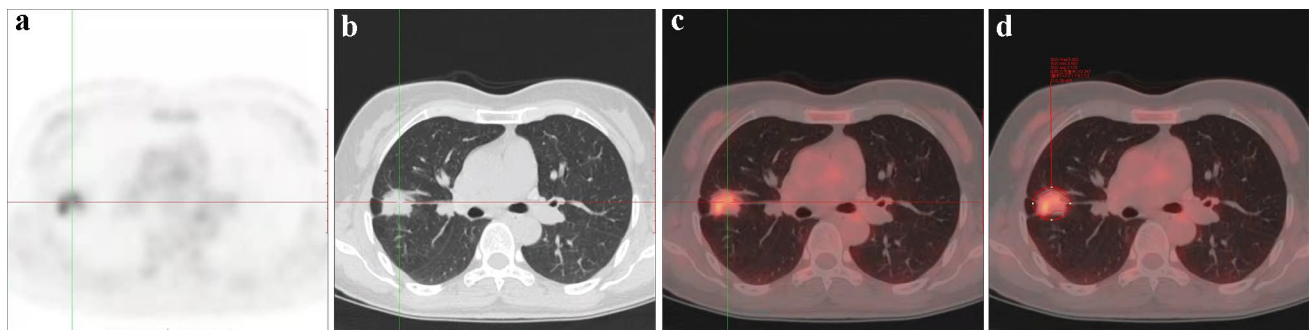


**Fig. 2** Representative $^{18}$F-FDG PET-CT images for EGFR mutation patients with NSCLC. A 47-year-old woman with a lesion in the upper lobe of the right lung, maximum diameter was approximately 27 mm, which was diagnosed pathologically as adenocarcinoma, and EGFR detection revealed an exon 19 deletion. FDG uptake was increased abnormally, corresponding SUVmax, SUVmean, and COV was 5.303, 3.116, and 199.81. Panels **a**, **b**, **c** and **d**: transverse PET, CT, PET/CT images, and ROI of the lesion, respectively
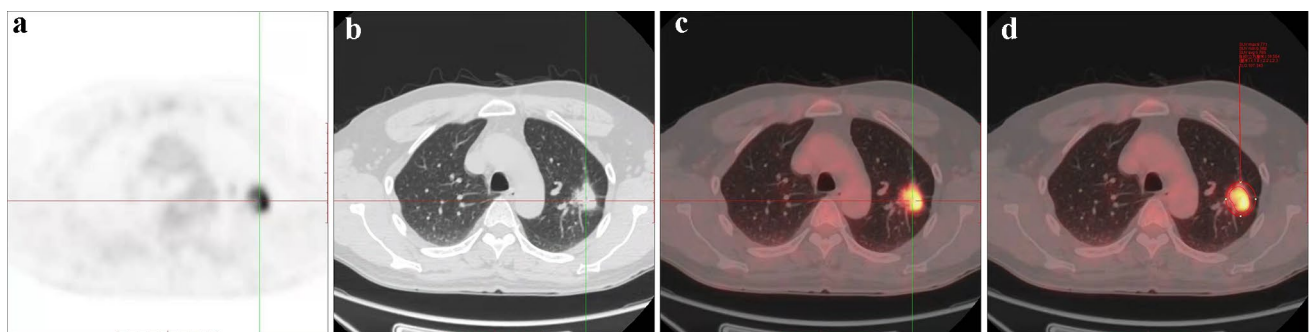


**Fig. 3** Representative $^{18}$F-FDG PET-CT images for EGFR wide-type patients with NSCLC. A 45-year-old man with a lesion in the upper lobe of the left lung, maximum diameter was approximately 25 mm, which was diagnosed pathologically as adenocarcinoma, and EGFR detection revealed no positive mutation. FDG uptake was increased abnormally, corresponding SUVmax was 9.771, 5.785, and 102.29. Panels **a**, **b**, **c** and d: transverse PET, CT, PET/CT images, and ROI of the lesion, respectively

fluids to analyze the status of EGFR mutations is susceptible to specimen limitations, preventing some patients from benefiting. Although there is evidence that clinical features such as adenocarcinoma, female gender, non-smoking status, and Asian regions are associated with EGFR mutations, more accurate predictive factors have yet to be discovered. Previous studies have reported that EGFR could affect cell membrane glucose transporters through downstream pathways, which in turn affects tumor glucose metabolism [11]. $^{18}$F-FDG PET/CT has the ability to reflect intratumoral glucose metabolism in a non-invasive way; as a result, it has gradually gained more attention.

In this study, the EGFR mutation rate was 56%, which was consistent with a previous report on Asian populations (36.8–76.2%). Univariate analysis showed that sex, smoking history, pathological type, tumor location, maximum diameter, T stage, SUVmax (P = 0.038), SUVmean (P = 0.038), MTV (P = 0.002), TLG (P = 0.002), and COV (P = 0.004) were significantly associated with EGFR mutations. Multivariate logistic regression analysis showed that only non-smokers, peripheral lung cancer, low SUVmax (≤ 7.85), low SUVmean (≤ 5.34), and high COV (≥ 106.08) were independent predictors, and it was favorable to distinguish EGFR mutation status when combining these factors to construct the corresponding model. In addition, the results were further stratified according to specific EGFR mutation subtypes. Because the majority of patients in our cohort had exon 19 or 21 mutations, FDG uptake was compared between the wild-type group and L858R in exon 21 or in-frame deletion in exon 19, and there was no significant difference, which is consistent with previous studies [20, 22].

Previous studies based on SUVmax to predict EGFR mutations have shown conflicting results. Most studies have shown that a low SUVmax is associated with EGFR mutations [12, 13], and the optimal threshold range was 2.69–11.5. Gu et al. [14] included 210 cases of stage I–IV NSCLC and showed that a low SUVmax (< 9.0) was significantly associated with mutations. Some studies included only stage IIIB and IV patients and found that a low SUVmax (< 9.6) might be a predictor of EGFR mutation [15]. These observations are consistent with the present study (SUVmax ≤ 7.85), but the thresholds varied. Patients with advanced stages of cancer appear to have slightly higher thresholds. The reason may be partially explained by the statement reported in the previous literature that the heterogeneity of the tumors carrying mutations may alter during cloning and evolution, resulting in consequent changes in metabolic characteristics [16]. Furthermore, the molecular mechanisms between SUVmax and EGFR mutation were explored, and the investigators discovered that the NADPH oxidase 4 (NOX4)/reactive oxygen species (ROS)/cellular membrane glucose transporter protein 1 (GLUT1) axis plays an important role in glucose metabolism, and ROS activity

is reduced when NOX4 expression is downregulated, leading to decreased GLUT1 expression. The mutant tumor cells have lower ROS activity, thus explaining the reduced uptake of $^{18}$F-FDG in EGFR-mutant cells to some degree [17]. However, a few studies have drawn the opposite conclusion that higher SUVmax was more prone to mutation [18], with the optimal threshold range being 5.0–13.65. Ko et al. [19] showed that patients with an SUVmax ≥ 6 had a higher frequency of mutations. Wang et al. [20] observed a significant increase in glucose uptake and lactate production in mutant NSCLC compared to the wild type, which explains the reason for higher SUVmax in mutant patients. Moreover, some studies did not find a correlation between the two [21].

Since SUVmax only reflects the highest FDG uptake value of a single pixel within the lesion, some studies started to take other parameters into consideration to reflect the metabolic behavior more comprehensively, suggesting that neither MTV nor TLG had a predictive value for EGFR mutations, which is consistent with some current studies [22, 23]. Similar results were observed in the study by Whi et al. [24], in which univariate analysis showed that SUVmax, MTV, and TLG were significantly associated with EGFR mutations, but after multivariate analysis, low SUVmax was the sole predictor, whereas MTV and TLG could not independently predict EGFR mutations.

The controversy regarding the correlation between metabolic parameters and EGFR mutation status may be attributed to the following reasons. First, the metabolic parameters SUVmax and SUVmean are influenced by various factors, such as patient characteristics and technique, and SUVmax sometimes does not reflect the integral characteristics of the tumor. Second, study design, patient selection, pathological type, and cancer stage may also influence the results. Third, other types of mutations may also affect glucose metabolism and cause differences in the results [25].

To reflect intratumor metabolic heterogeneity more accurately, this study included COV as a heterogeneity index and found that it could independently predict EGFR mutations and that patients with higher COV were more likely to have mutations. Some scholars used 1/COV to analyze the relationship, and univariate analysis revealed that patients with high 1/COV were prone to mutation, but multivariate analysis failed to predict it independently. The reason the results were different from those of this study may be attributed to the racial differences of the included patients and the mutation rate; all patients were from the United States, with a 25.2% mutation rate in the latter study. Thus, it is necessary to conduct multi-ethnic and larger studies to explore the relationship between tumor heterogeneity parameters and EGFR mutations [22].

In this study, AUC of the metabolic and heterogeneity parameters was analyzed using ROC curves, and the predictive efficacy of TLG was the highest. After multivariate

analysis, SUVmax, SUVmean, and COV could predict EGFR mutations, with the latter two having better predictive efficacy than SUVmax, while MTV and TLG failed to predict independently, which may be related to the intrinsic characteristics of these parameters. SUVmean is the average SUV within the ROI and reflects more metabolic information. MTV and TLG tend to reflect the whole tumor metabolism and are susceptible to FDG uptake and tumor volume, whereas COV is unaffected by tumor volume. Zhang et al. [26] found that the AUCs of SUVmax and SUVmean to identify EGFR mutations were 0.629 and 0.632, respectively, which is similar to the results of the present study. Notably, the present study revealed that the individual predictive efficacy of smoking history was higher than that of SUVmax and SUVmean, with an AUC of 0.711 for the former, and the individual predictive efficacy of tumor location was lower, with an AUC of 0.620, but both were lower than that of COV. This implies that the metabolic parameters showed moderate predictive efficacy, while tumor heterogeneity parameters showed superior predictive efficacy, suggesting that COV has potential application value. Guo et al. [27] included 18 relevant pieces of literature for meta-analysis, suggesting that SUVmax and SUVmean showed moderate predictive ability for mutation, supporting the results of this study. On combining these five factors to construct a prediction model, the AUC reached 0.926, and the predictive efficacy was higher than that of a single parameter. The corresponding sensitivity, specificity, positive predictive value, negative predictive value, and percentage correct were 96.4%, 83.7%, 89.1%, 86.0%, and 87.8%, respectively, indicating that the model has good predictive efficacy and accuracy and can help guide EGFR-mutant patients for EGFR–TKI-targeted therapy.

Some clinical characteristics were also included in this study. As shown in most previous research, there were significant differences in EGFR status among women, non-smokers, and patients with adenocarcinoma. The maximum tumor diameter ($\leq 3.4$ cm) was significantly associated with mutations, and similar results were observed in previous studies [13]. Liu et al. [28] showed that peripheral lung cancer is prone to mutation, which is consistent with the results of this study, indicating an association between tumor location and internal metabolism. However, there have been few studies involving this factor, and large-scale studies are necessary to elucidate it. In addition, CT marginal signs were not associated with mutations, which is consistent with previously reported findings.

The novelty of this study lies in the synthesis of multiple metabolic and heterogeneity parameters of $^{18}$F-FDG PET/CT and the modeling performed to provide additional details regarding the intratumoral metabolic state. The study, however, has some limitations. First, this was a retrospective study with a small sample size, which may have caused selection bias. Furthermore, the small number of different mutant subtypes makes it difficult to draw definite conclusions. Second, other genetic alterations that may affect FDG uptake, such as ALK rearrangement, have not yet been analyzed because of their rarity. Third, in view of the different characteristic of the whole-body PET/CT scanning and general CT plain scanning, the clarity of lung lesions in PET/CT obtained is not as good as plain chest CT alone in practical work, so ground glass opacities (GGO) has not been taken into consideration to avoid the inaccuracy of its evaluation, which may lead to inadequate research. However, the value of GGO for the study of EGFR mutations cannot be denied [29, 30], using a larger sample size to attempt to conduct more related studies in the future is necessary. In addition, the prediction model has not yet been validated, and the prognosis remains unclear. Further exploration to consider these deficiencies will be significant in the future.

In conclusion, this study showed that smoking history, tumor location, SUVmax, SUVmean, and heterogeneity parameter COV are independent predictors of EGFR mutation, and combining them to build a model that demonstrated better predictive efficacy is conducive to distinguishing the mutation status of patients who fail to undergo EGFR testing and guide EGFR–TKI-targeted therapy. Future prospective and large-scale investigations are required to confirm the predictive value of $^{18}$F-FDG PET/CT metabolism-related information for EGFR mutations.

**Data availability** All data generated or analyzed during this study are included here.

## Declarations

**Conflict of interest** The authors declare that they have no conflicts of interest.

**Ethical approval** This article does not contain any studies with animals performed by any of the authors. All procedures performed in studies involving human participants were in accordance with the ethical standards of the institutional and/or national research committee and with the principles of the 1964 Declaration of Helsinki and its later amendments or comparable ethical standards.

**Informed consent** Informed consent was obtained from the patients for the anonymous use of the clinical, imaging, and histological data for publication.

# References

1. Erratum: Global cancer statistics 2018: GLOBOCAN estimates of incidence and mortality worldwide for 36 cancers in 185 countries. CA Cancer J Clin. 2020;70(4): 313.
2. Bousquet Mur E, Bernardo S, Papon L, Mancini M, Fabbrizio E, Goussard M, et al. Notch inhibition overcomes resistance to tyrosine kinase inhibitors in EGFR-driven lung adenocarcinoma. J Clin Invest. 2020;130(2):612–24.
3. An N, Zhang Y, Niu H, Li Z, Cai J, Zhao Q, et al. EGFR-TKIs versus taxanes agents in therapy for nonsmall-cell lung cancer patients: A PRISMA-compliant systematic review with meta-analysis and meta-regression. Medicine. 2016;95(50):e5601.
4. McGranahan N, Swanton C. Clonal heterogeneity and tumor evolution: past, present, and the future. Cell. 2017;168(4):613–28.
5. Van Baardwijk A, Bosmans G, van Suylen RJ, van Kroonenburgh M, Hochstenbag M, Geskes G, et al. Correlation of intra-tumour heterogeneity on 18F-FDG PET with pathologic features in non-small cell lung cancer: a feasibility study. Radiother Oncol. 2008;87(1):55–8.
6. Moon SH, Cho YS, Son YI, Ahn YC, Ahn MJ, Choi JY, et al. Value of 18F-FDG heterogeneity for discerning metastatic from benign lymph nodes in nasopharyngeal carcinoma patients with suspected recurrence. Br J Radiol. 2016;89(1067):20160109.
7. Pahk K, Chung JH, Yi E, Kim S, Lee SH. Metabolic tumor heterogeneity analysis by F-18 FDG PET/CT predicts mediastinal lymph node metastasis in non-small cell lung cancer patients with clinically suspected N2. Eur J Radiol. 2018;106:145–9.
8. Yoon HJ, Kim Y, Kim BS. Intratumoral metabolic heterogeneity predicts invasive components in breast ductal carcinoma in situ. Eur Radiol. 2015;25(12):3648–58.
9. Watabe T, Tatsumi M, Watabe H, Isohashi K, Kato H, Yanagawa M, et al. Intratumoral heterogeneity of F-18 FDG uptake differentiates between gastrointestinal stromal tumors and abdominal malignant lymphomas on PET/CT. Ann Nucl Med. 2012;26(3):222–7.
10. Goldstraw P, Chansky K, Crowley J, Rami-Porta R, Asamura H, Eberhardt WE, et al. The IASLC lung cancer staging project: proposals for revision of the TNM stage groupings in the Forthcoming (Eighth) Edition of the TNM Classification for lung cancer. J Thorac Oncol. 2016;11(1):39–51.
11. Kaira K, Serizawa M, Koh Y, Takahashi T, Yamaguchi A, Hanaoka H, et al. Biological significance of 18F-FDG uptake on PET in patients with non-small-cell lung cancer. Lung Cancer. 2014;83(2):197–204.
12. Na II, Byun BH, Kim KM, Cheon GJ, Choe DH, Koh JS, et al. 18F-FDG uptake and EGFR mutations in patients with non-small cell lung cancer: a single-institution retrospective analysis. Lung Cancer. 2010;67(1):76–80.
13. Guan J, Xiao NJ, Chen M, Zhou WL, Zhang YW, Wang S, et al. 18F-FDG uptake for prediction EGFR mutation status in non-small cell lung cancer. Medicine. 2016;95(30):e4421.
14. Gu J, Xu S, Huang L, Wu J, Xu J, Feng J, et al. Value of combining serum carcinoembryonic antigen and PET/CT in predicting EGFR mutation in non-small cell lung cancer. J Thorac Dis. 2018;10(2):723–31.
15. Hong IK, Lee JM, Hwang IK, Paik SS, Kim C, Lee SH, et al. Diagnostic and predictive values of 18F-FDG PET/CT metabolic parameters in EGFR-mutated advanced lung adenocarcinoma. Cancer Manag Res. 2020;12:6453–65.
16. Kohsaka S, Petronczki M, Solca F, Maemondo M. Tumor clonality and resistance mechanisms in EGFR mutation-positive non-small-cell lung cancer: implications for therapeutic sequencing. Future Oncol. 2019;15(6):637–52.
17. Chen L, Zhou Y, Tang X, Yang C, Tian Y, Xie R, et al. EGFR mutation decreases FDG uptake in non-small cell lung cancer via the NOX4/ROS/GLUT1 axis. Int J Oncol. 2019;54(1):370–80.
18. Huang CT, Yen RF, Cheng MF, Hsu YC, Wei PF, Tsai YJ, et al. Correlation of F-18 fluorodeoxyglucose-positron emission tomography maximal standardized uptake value and EGFR mutations in advanced lung adenocarcinoma. Med Oncol. 2010;27(1):9–15.
19. Ko KH, Hsu HH, Huang TW, Gao HW, Shen DH, Chang WC, et al. Value of $^{18}$F-FDG uptake on PET/CT and CEA level to predict epidermal growth factor receptor mutations in pulmonary adenocarcinoma. Eur J Nucl Med Mol Imaging. 2014;41(10):1889–97.
20. Wang Y, Han R, Wang Q, Zheng J, Lin C, Lu C, et al. Biological significance of 18F-FDG PET/CT maximum standard uptake value for predicting EGFR mutation status in non-small cell lung cancer patients. Int J Gen Med. 2021;14:347–56.
21. Lee SM, Bae SK, Jung SJ, Kim CK. FDG uptake in non-small cell lung cancer is not an independent predictor of EGFR or KRAS mutation status: a retrospective analysis of 206 patients. Clin Nucl Med. 2015;40(12):950–8.
22. Minamimoto R, Jamali M, Gevaert O, Echegaray S, Khuong A, Hoang CD, et al. Prediction of EGFR and KRAS mutation in non-small cell lung cancer using quantitative 18F FDG-PET/CT metrics. Oncotarget. 2017;8(32):52792–801.
23. Kim YI, Paeng JC, Park YS, Cheon GJ, Lee DS, Chung JK, et al. Relation of EGFR mutation status to metabolic activity in localized lung adenocarcinoma and its influence on the Use of FDG PET/CT parameters in prognosis. Am J Roentgenol. 2018;210(6):1346–51.
24. Whi W, Ha S, Bae S, Choi H, Paeng JC, Cheon GJ, et al. Relationship of EGFR mutation to glucose metabolic activity and asphericity of metabolic tumor volume in lung adenocarcinoma. Nucl Med Mol Imaging. 2020;54(4):175–82.
25. Steuer CE, Behera M, Berry L, Kim S, Rossi M, Sica G, et al. Role of race in oncogenic driver prevalence and outcomes in lung adenocarcinoma: results from the Lung Cancer Mutation Consortium. Cancer. 2016;122(5):766–72.
26. Zhu L, Yin G, Chen W, Li X, Yu X, Zhu X, et al. Correlation between EGFR mutation status and F18 -fluorodeoxyglucose positron emission tomography-computed tomography image features in lung adenocarcinoma. Thorac Cancer. 2019;10(4):659–64.
27. Guo Y, Zhu H, Yao Z, Liu F, Yang D. The diagnostic and predictive efficacy of 18F-FDG PET/CT metabolic parameters for EGFR mutation status in non-small-cell lung cancer: a meta-analysis. Eur J Radiol. 2021;141:109792.
28. Liu A, Han A, Zhu H, Ma L, Huang Y, Li M, et al. The role of metabolic tumor volume (MTV) measured by [18F] FDG PET/CT in predicting EGFR gene mutation status in non-small cell lung cancer. Oncotarget. 2017;8(20):33736–44.
29. Hong SJ, Kim TJ, Choi YW, Park JS, Chung JH, Lee KW. Radiogenomic correlation in lung adenocarcinoma with epidermal growth factor receptor mutations: Imaging features and histological subtypes. Eur Radiol. 2016;26(10):3660–8.
30. Sugano M, Shimizu K, Nakano T, Kakegawa S, Miyamae Y, et al. Correlation between computed tomography findings and epidermal growth factor receptor and KRAS gene mutations in patients with pulmonary adenocarcinoma. Oncol Rep. 2011;26(5):1205–11.